9th ANKARA INTERNATIONAL AEROSPACE CONFERENCE **AIAC-2017-076**
20-22 September 2017 - METU, Ankara TURKEY

STATİC AEROELASTİC RESPONSE PREDİCTİON OF TRANSPORT AİRCRAFT USİNG COUPLED CFD/CSD METHOD

Haris Hameed Mian[1], Hasan Junaid Hasham[2],
Jawad Khawar[3], Khurram Nisar[4]
Center of Excellence in Sciences and Applied Technologies (CESAT)
Islamabad, Pakistan

Wang Gang[5], ZhengYin Ye[6]
School of Aeronautics, Northwestern Polytechnical University
Xian, P.R. China

ABSTRACT

Numerical estimation of aerodynamic loads of transport aircraft configurations considering the static aeroelastic deformations at steady-state conditions is presented. Fluid-structure coupled simulations using high fidelity fluid dynamic and structural analysis solvers have been applied to study aeroelastic response of DLR-F11 high-lift configuration and a research civil transport aircraft (RCTA) model. Static aeroelastic simulations were performed by developing a partitioned coupling procedure linking a RANS based in-house flow solver HUNS3D and an open source finite element solver CalculiX. Radial basis function interpolation technique has been used to map data between the non-conformal meshes and to deform the CFD volume mesh. To validate the numerical results, the predicted aerodynamic data for the rigid model was compared with the experimental data and good agreement was obtained. Coupled simulations were performed for DLR-F11 model at Mach 0.2 at several load factors. The results showed that even at low speed the deformation of the model is not negligible. The predicted wing tip deformation and the gap variation between the main wing and the flap were in accordance with the experimentally measured values. For RCTA model simulations were performed at Mach 0.78 at various angles of attack. The lift curve slopes obtained for rigid and elastic models were compared with the experimental data. It was observed that the elastic model results correspond well with the measured values. The results show that the developed coupling procedure is robust and accurate for complex aircraft configurations.

INTRODUCTION

Over the recent years computational aeroelastic simulations have gained a lot of interest owing to the significant improvements made in the field of computational fluid dynamics (CFD), computational structural dynamics (CSD) and computing technologies [Bennett and Edwards,1998]. For aerodynamic design process CFD analysis has become an imperative

[1] Researcher, Email: harishameed_33@hotmail.com
[2] Phd Researcher , Email: hjhasham@yahoo.com
[3] Phd Researcher , Email: newworld11@yahoo.com
[4] Phd Researcher
[5] Phd, Associate Professor, wanggang@nwpu.edu.cn
[6] Phd, Professor, School of Aeronautics

part and is now efficiently included in the initial design and analysis phase. The aerodynamic performance of large transport aircrafts depends on the deformation of their wings. In many cases the structural deformations caused by the aerodynamic loads significantly affect the surrounding fluid and thus cannot be neglected. In this situation, even the mono-disciplinary CFD approaches become insufficient for accurate and high quality numerical prediction of the aerodynamic data [Keye and Rudnik,2009]. Therefore precise validation of the numerical flow simulation requires the interaction between the fluid flow and the elastic structure.

Three different CFD/CSD coupling approaches have been adopted and explained in literature: fully coupled, closely coupled and loosely coupled approach. In fully coupled (also known as strong/tight/monolithic coupling approach), the governing equations for both the structure and fluid are combined into a single set and are solved simultaneously [Guruswamy,2009]. Closely coupled approach is usually not regarded as a separate method, rather a type of the loosely coupled approach. Wherein, the fluid and structure modules are developed separately but are combined in one single module by some interfacing technique [Guruswamy,2009]. As for the loosely coupled (also known as partitioned approach), the fluid and the structure parts are treated and solved separately and the interaction between them is external only [Bhardwaj, Kapania, Reichenbach, and Guruswamy,1998]. The advantage of using the fully coupled method is that the computational results can be obtained in a single analysis. However, this method needs extensive modification to couple the fluid and structure codes. Also it is restricted to two-dimensional problems and some small scale three dimensional systems. On the contrary, the loosely coupled approach can be developed without any modifications in the existing fluid and the structure solvers. Using this approach, the computational aeroelastic analysis can be performed using any aerodynamic and structural analysis codes with some modification. This approach has been used in the present work to couple the existing three dimensional finite volume based hybrid unstructured Navier-Stokes flow solver HUNS3D [Mian, Wang and Raza, 2013] with an open source finite element suit CalculiX [Dhondt, 2012].

The coupling approach is designed to simulate static aeroelastic effects only. Key requirements for loose coupling approach are an efficient interpolation method for two-way data transfer and a mesh deformation scheme. Previously, different techniques have been proposed and implemented to get high quality deformed meshes for unstructured or hybrid-unstructured meshes. These include spring analogy method [Batina, 1991], linear elasticity analogy [Huo, Wang, Yan and Yue, 2010], Delaunay graph mapping [Liu, Qin, Xia, 2006] and a meshless method for grid deformation based on the multivariate interpolation using radial basis functions (RBF) [Rendall, 2010]. RBF interpolation method is independent of grid type, accounts for surface rotations and preserves grid orthogonality. This method has been used here for both the two-way data interpolation and CFD volume mesh deformation. The efficiency of this method has been enhanced by using improved data reduction schemes based on “double edge” greedy algorithm [Wang, Mian, Ye, and Lee, 2013]. The results of this method has shown that RBF mesh deformation provides good quality mesh motion even for large boundary motion and is suitable for any type of mesh (structured or unstructured).

In this paper the developed CFD/CSD coupled environment has been used to investigate the static aeroelastic behavior of complex civil transport aircraft configurations. These include DLR-F11 high-lift model in landing configuration [HiLiftPW-2, 2013] and research civil transport aircraft (RCTA) model. Different test conditions have been simulated for both the configurations and the predicted results were compared with the available experimental data. The paper starts out by introducing briefly the CFD and CSD solvers and the radial basis function interpolation technique. Next, the numerical models used for CFD and CSD simulations are described and the coupled simulation details are discussed. Finally the numerical results for the static aeroelastic analysis and some concluding remarks are presented.

CFD /CSD SOLVERS

The two main driving components of computational aeroelasticity are the fluid dynamics and the structure dynamics solver. Both the solvers are defined by their own principles and have different governing equations. Brief introduction of the CFD and CSD solvers used in this work is described here.

CFD Solver

HUNS3D flow solver solves the full three-dimensional compressible Reynolds-Averaged Navier-Stokes (RANS) equations using cell-centered finite volume method on unstructured hybrid meshes composed of hexahedrons, prisms, tetrahedrons and pyramids. The solver is equally capable to perform numerical computations on structured grids. The code has been developed by fluid dynamics department of Northwestern Polytechnical University. Several upwind or central convective flux discretization schemes are available in this flow solver [Wang and Ye, 2004]. The semi-discretized equations are integrated implicitly by the backward Euler method together with improved LU-SGS scheme [Gang, Jiang and Ye, 2012]. This code has been parallelized with OpenMP in globally shared memory model. A choice of turbulence models is available in the code including the one-equation Spalart-Allmaras (S-A) model, two-equation Shear Stress Transport (SST) k-ω model and hybrid RANS-LES (DES) model. HUNS3D flow solver is a complete system for the prediction of viscous and inviscid flows about complex geometries from the low subsonic to the hypersonic flow regime, employing hybrid unstructured grids.

CSD Solver

For the structure dynamics solution an open source three dimensional finite element based solver CalculiX [Dhondt, 2012] has been used to get the structural displacements. The solver is capable of performing linear and non-linear calculations and handling a wide variety of mechanical, thermal, coupled thermo-mechanical, and contact problems. There is a graphics pre/post-processor program GraphiX (cgx) that supports the solver program, CalculiX (ccx). The input format of the solver is a similar to a well known commercial finite element analysis software ABAQUS®. This provides an added benefit of using commercial software suite as pre-processor. The solver can also work in parallel environment using either MPI or OpenMP support [HiLiftPW-2, 2012]. In this work the solver has been re-compiled to be able to work in Linux environment using OpenMP parallelization.

RADIAL BASIS FUNCTION INTERPOLATION

The form of required interpolation based on RBFs can be written as [Rendall and Allen, 2008]

$$F(\mathbf{r}) = \sum_{i=1}^{N} w_i \phi(\|\mathbf{r} - \mathbf{r}_i\|) \tag{1}$$

Where, $F(\mathbf{r})$ is the function to be evaluated at location $\mathbf{r}$ and it will be specified to represent the displacement of mesh points. $\varphi(\|\mathbf{r} - \mathbf{r}_i\|)$ is general form of some kind of RBF adopted, N is the number of RBFs involved in the interpolation and $\mathbf{r}_i$ is the location of the supporting centre for the RBF labeled with index i. The coefficients w_i can be determined by requiring exact recovery of the original function at N sample points. In this work, Wendland's C^2 function is selected as the basis function according to the work of Rendall and Allen [Rendall , 2008]. This function has the formulation of

$$\phi(\eta) = (1-\eta)^4 (4\eta + 1) \tag{2}$$

Where $\eta = \frac{\|\mathbf{r} - \mathbf{r}_i\|}{d}$ with d denotes the supporting radius of RBF series. The maximum value of η is limited to 1, which gives a zero value to a RBF at a large distance d. For mesh deformation, the supporting centre of RBF is located at the mesh points on the moving surface. The set of sample points used to determine the coefficients w_i is selected as the supporting centers of RBFs. This interpolation problem is described in the following matrix expressions.

$$\Delta \mathbf{X}_S = \mathbf{\Phi} \mathbf{W}_X \tag{3}$$

$$\Delta \mathbf{Y}_S = \mathbf{\Phi} \mathbf{W}_Y \tag{4}$$

$$\Delta \mathbf{Z}_S = \mathbf{\Phi} \mathbf{W}_Z \tag{5}$$

Where, $\Delta \mathbf{X}_S = \{\Delta x_{S_1}, \cdots, \Delta x_{S_N}\}^T$, $\Delta \mathbf{Y}_S = \{\Delta y_{S_1}, \cdots, \Delta y_{S_N}\}^T$ and $\Delta \mathbf{Z}_S = \{\Delta z_{S_1}, \cdots, \Delta z_{S_N}\}^T$ represents the displacement components of the surface mesh points with S denotes the boundary surface. Φ is the basis matrix. $\mathbf{W}_X = \{w^x_{S_1}, \cdots, w^x_{S_N}\}^T$, $\mathbf{W}_Y = \{w^y_{S_1}, \cdots, w^y_{S_N}\}^T$ and $\mathbf{W}_Z = \{w^z_{S_1}, \cdots, w^z_{S_N}\}^T$ are interpolation coefficients series need to be determined by solving Eq.(3-5). The displacements of volume nodes are calculated as the following formula

$$\Delta x_j = \sum_{i=S_1}^{S_N} w_i^x \phi(\|\mathbf{r}_j - \mathbf{r}_i\|) \quad ; \quad \Delta y_j = \sum_{i=S_1}^{S_N} w_i^y \phi(\|\mathbf{r}_j - \mathbf{r}_i\|) \quad ; \quad \Delta z_j = \sum_{i=S_1}^{S_N} w_i^z \phi(\|\mathbf{r}_j - \mathbf{r}_i\|) \qquad (j = 1, 2 \ldots N_V) \tag{6}$$

Here, N_V is the number of volume mesh nodes. The key process of RBF mesh deformation is to setup a RBF interpolation to describe the deformation of boundaries approximately. And the realization of this process is referred by constructing and solving the Eq. (3-5) efficiently.

To simplify expressions, Equations (3-5) are expressed in the following universal form

$$\Delta \mathbf{S} = \mathbf{\Phi} \mathbf{W} \tag{7}$$

In the above part, N surface points are used to establish the interpolation basis matrix $\mathbf{\Phi}$, which means that the computational cost of solving Eq.(7) is N^3 and a volume mesh update computational scale $N \times N_V$. For small to medium sized meshes, in which the number of surface points is relatively small, the full set of surface points can be taken as the sample points. While for large mesh cases, the number of surface points N often gets to hundreds of thousands. In such cases, the data reduction algorithm should be used to limit the size of RBF interpolation in a reasonable scale. To accomplish this error-driven data reduction greedy algorithm has been used . Since a surface mesh point uniquely corresponds to a support center of RBF, a surface point set $P^M = \{p_1, p_2, \ldots, p_M\}$ also uniquely determines a M dimension RBF function space $R^{(M)}$. Hence, the data reduction algorithm in RBF interpolation is actually a selection process to obtain a subset P^M from the full surface mesh point set P^N, and use P^M instead of P^N as the support center to establish a smaller dimensional RBF interpolation.

To improve the above data reduction process, a multi-level subspace RBF interpolation based on “double-edge” greedy algorithm [Wang, Mian, Ye and Lee, 2013] has been used. In classical greedy method only one point that has the largest error is selected. But in double edge greedy method, once the point has maximal, the magnitude of error is found by scanning over the surface mesh points and the direction of the error on this point is determined. Then a secondary scan is made to find another point that has the largest error. In this way two points are selected in a single greedy iteration. If M points were finally selected by adding single point in each greedy iteration, then the computational cost of solving Eq. (7) has the order M^3 and this equation is to be solved M times thus the cost of constructing the final RBF interpolation is M^4. While by using the double edge method and selecting two points in each greedy cycle the computational cost of forming the RBF interpolation with M points is reduced to about $M^4/8$. This technique has been further improved by designing a multi-level subspace RBF interpolation [Wang, Mian, Ye and Lee, 2013]. If a number of M points are specified for each level, then the computational cost of constructing a RBF interpolation with $10 \times M$ supporting points is in the order of $10 \times M^4$, which was $(10 \times M)^4$ for classical method with same supporting points.

NUMERICAL MODELS

DLR-F11 high-lift configuration

The high lift configuration model was presented as a test case for the 2nd AIAA CFD High Lift Prediction Workshop (HiliftPW-2) [HiLiftPW-2, 2013] to assess the performance of CFD codes for numerical prediction of aerodynamic data for complex configurations. From meshing to computational analysis, these complex configurations are challenging for both the fluid and structure dynamics fields. The DLR-F11 model in high-lift landing configuration consists of a fuselage and a three-element wing (the main wing, a full-span slat, a full-span flap, slat brackets and flap fairings). It has a length of approx. 2.8m, a semi-span of 1.4m, a mean aerodynamic chord of 0.347m, quarter chord sweep of 30^{o} and the fuselage length of 3.077 m. The planform view with key dimensions highlighted and the wind tunnel model are shown in (Figure. 1 (a) and (b)), respectively. The material properties of steel with Elastic modulus of 200 GPa, Poisson's ratio of 0.3 and material density of 7860 Kg/m^3 were used.

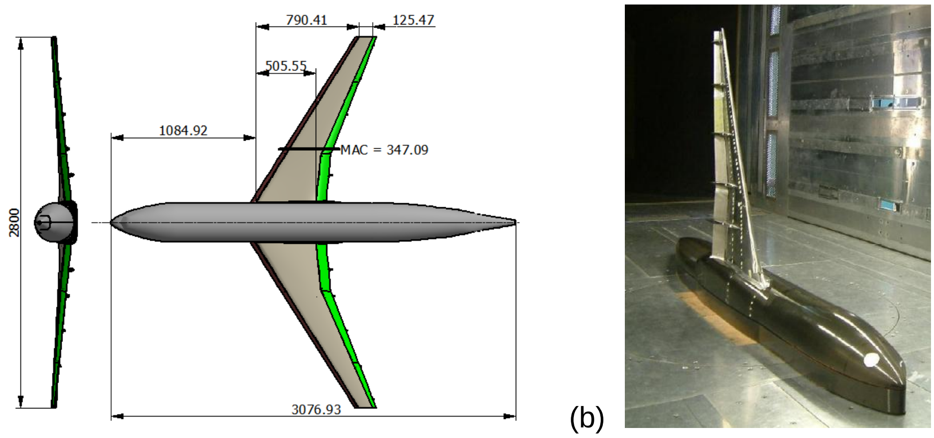

(a) (b)

Figure 1 : (a) Planform view of DLR – F11 (b) Wind tunnel model

Hybrid unstructured CFD volume mesh and unstructured finite element model have been generated for this configuration, as shown in (Figure 2 (a) and (b)), respectively. CFD mesh contains mixtures of tetrahedral, pyramids and 28 layers of prism cells in the boundary layer region. The mesh has 149789 surface mesh points, 4455594 mesh nodes and 12554672 volume cells. In comparison to that, the finite element model consists of 112059 volume nodes and 56583 surface mesh points. The element type for CSD grid is C3D10 which is a quadratic element used for tetrahedral meshes. The advantage of these meshes is that they can be used to model complex solid geometries without modifying the geometry. The CFD/CSD mesh overlap has been illustrated in (Figure 2 (c)). Different CFD and CSD meshes have been generated to ascertain that the results are independent of the mesh size.

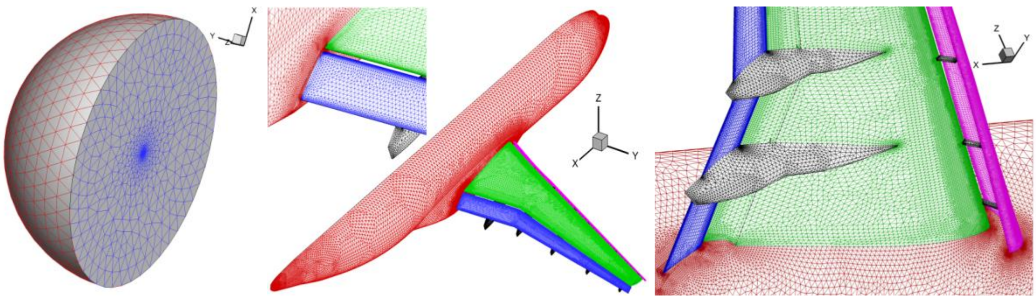

(a)

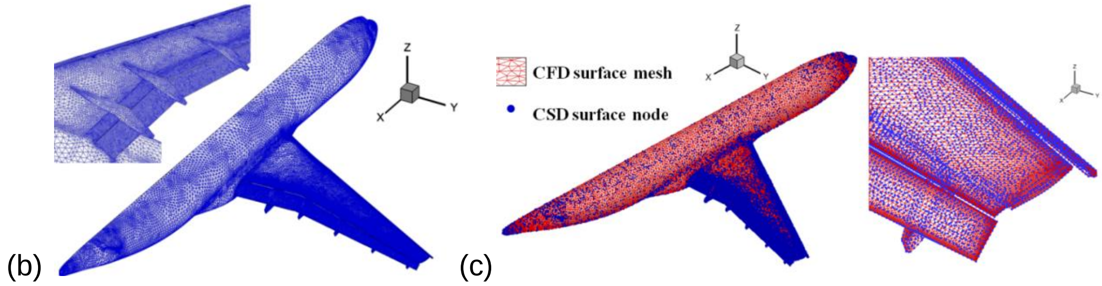

Figure 2 : (a) Hybrid unstructured CFD mesh details (b) Tetrahedral CSD mesh (c) CFD/CSD mesh overlap

Research civil transport aircraft (RCTA) model

The RCTA model (planform view shown in Figure 3 (a)) was tested to get aerodynamic data in transonic flow regime and study design characteristics of a research model. Hybrid-unstructured mesh with 13930874 cells, 4906865 volume nodes and 28 layers of prism mesh in boundary layer was generated for CFD computations. The structural model is generated with 362643 tetrahedral elements and 558101 node points. The CFD surface mesh of RCTA model is shown in Figure 3 (b). The finite element model for CSD computations is shown in Figure 3 (c). The CFD/CSD mesh overlap has been illustrated in Figure 3 (d). Different CFD and CSD meshes have been generated to ascertain that the results are independent of the mesh size.

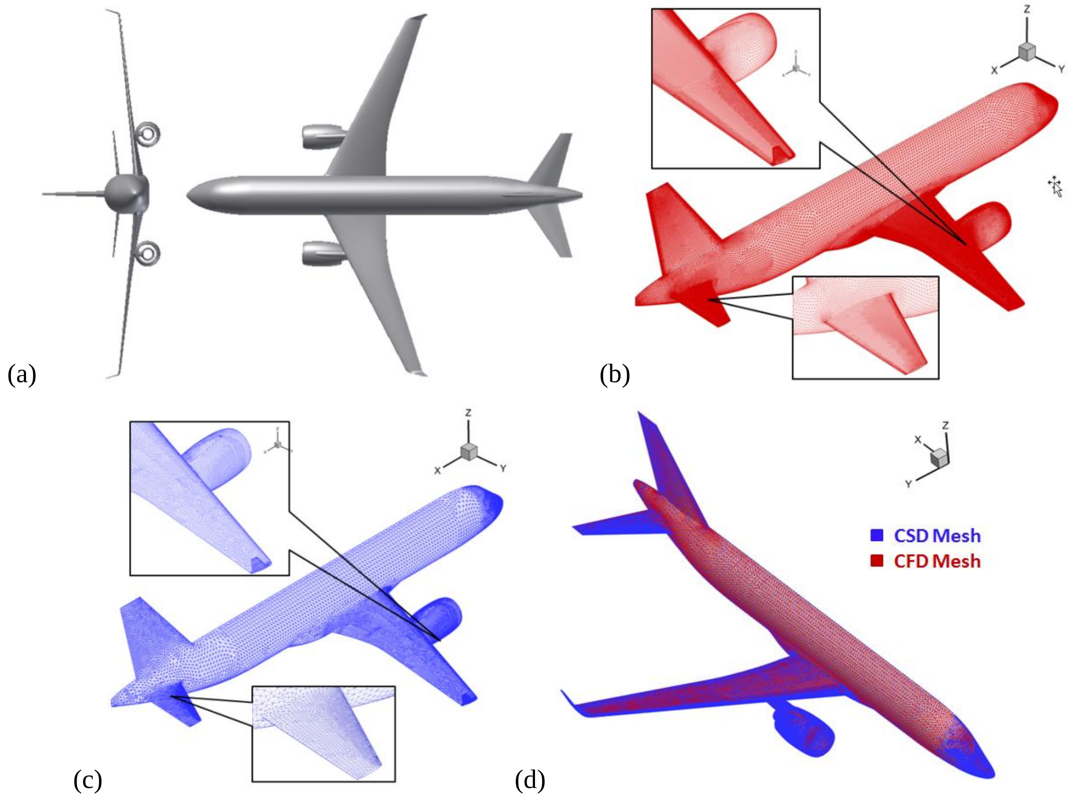

Figure 3 : RCTA model and computational mesh (a) Planform view (b) Hybrid-unstructured CFD mesh (c) Tetrahedral CSD mesh (d) CFD/CSD mesh overlap

CFD/CSD COUPLED SIMULATIONS

(Figure 4) details the static aeroelastic coupling procedure adopted to accomplish aeroelastic equilibrium.

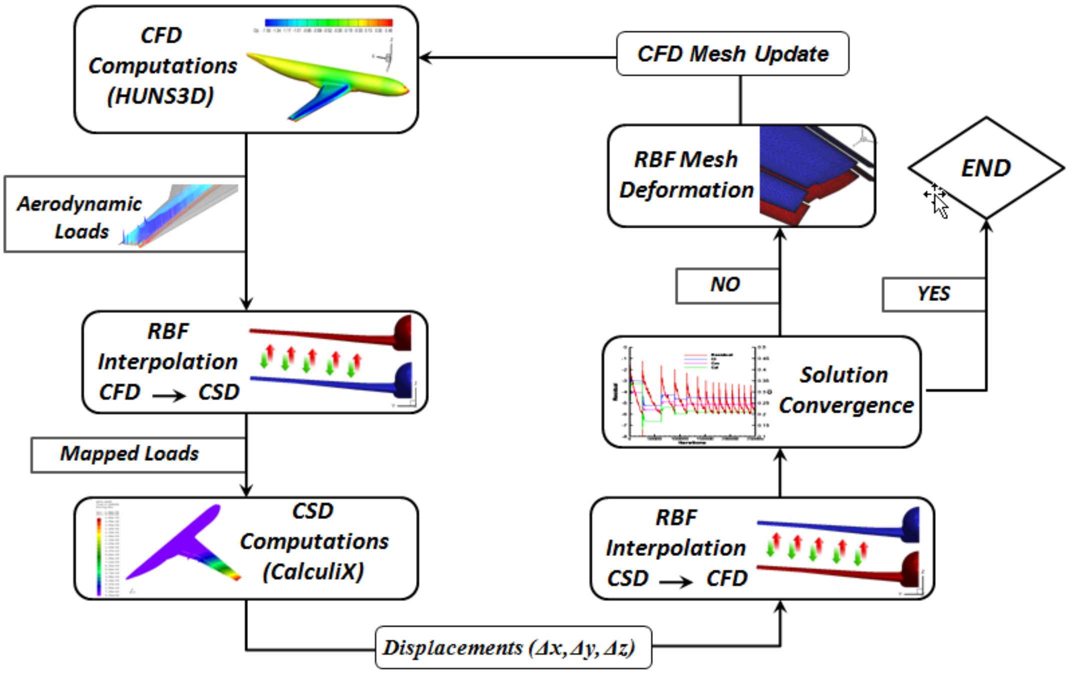

Figure 4 : CFD/CSD coupling profess for static aeroelastic analysis

As an initial step unreformed CFD volume mesh is used to obtain a converged solution. Then the aerodynamic loads predicted in the first step are mapped on the CSD surface mesh. This interpolation of loads is achieved by using RBF interpolation, which will be discussed in latter section. After transferring the loads from CFD surface to CSD surface the first CSD simulation is performed. CSD solver computes the deformation produced due to the applied load and then output this nodal deformation. This predicted deformation is then transferred back to deform the CFD volume mesh. This transfer is again achieved by using RBF data interpolation scheme. The new deformed CFD volume mesh and the previously converged CFD solution are then used to perform second CFD computation. This process is then repeated again and again until some aeroelastic equilibrium has been achieved or the user defined coupling iterations have been performed. Also the aerodynamic coefficients are compared for the last and previous coupling iteration. If the change in their values is smaller than the specified value then the coupling process is stopped and the static aeroelastic equilibrium is presumed to be reached

STATIC AEROELASTIC ANALYSIS RESULTS

DLR-F11 high-lift configuration

Although the main focus of presenting this configuration in HiliftPW-2 was to assess the meshing, turbulence modeling numerics, high-performance computing etc. for CFD codes but some experimental investigations was also performed to measure the deformation produced during the wind tunnel testing. Kirmse [Kirmse, 2007] published the experimental measurements made during the testing of DLR-F11 model. These measurements include the determination of bend and twist of the main wing together with the measurement of the gap between the main wing and the slat or the flap. These test showed that even for low speed testing and rigid models the deformation is not negligible. Moreover, the gap decrease of 10% was observed at the wing tip. Rudnik et al. [Rudnik, Huber and Melber-Wilkending,, 2012] suggested adding the static aeroelastic effects for wind tunnel measurement of DLR-F11 configuration. In this work static aeroelastic deflections are determined by changing the load factor. RBF interpolation procedure works well for even such large degree of freedom problems. The predicted and the mapped pressure distribution over the complete aircraft are shown in (Figure 5 (a) and (b)), respectively. The pressure interpolation was successful in transferring the pressure loads form CFD surface mesh to CSD surface mesh.

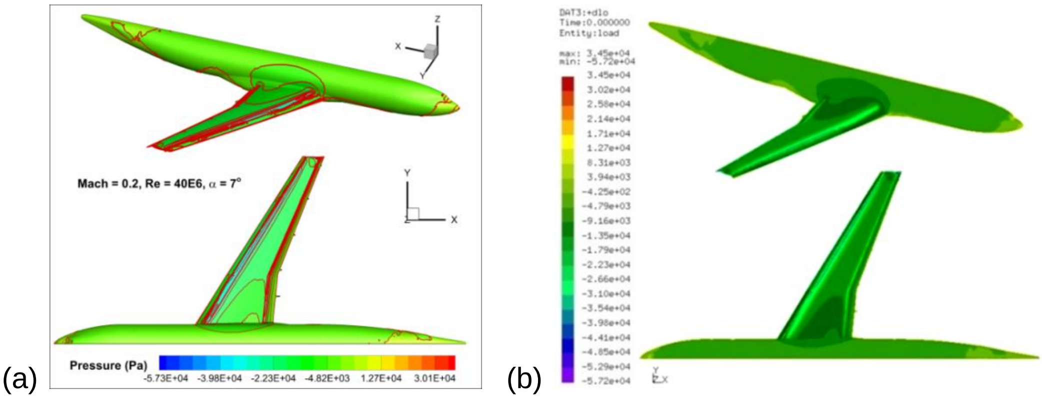

Figure 5 : (a) Pressure contours computed by CFD analysis (b) Mapped pressure load on CSD surface

The high-lift configuration was analyzed at Mach number 0.176, Reynolds number of 15.1 million, angle of attack of 7^{o} and for three different load factors (0.33E-7, 0.64E-7 and 0.84E-7). The wing tip displacement for the three loading conditions is shown in (Figure 6a). As it can be seen from the figure that even for a solid wing model, with material properties of structural steel, the deformations are not negligible.

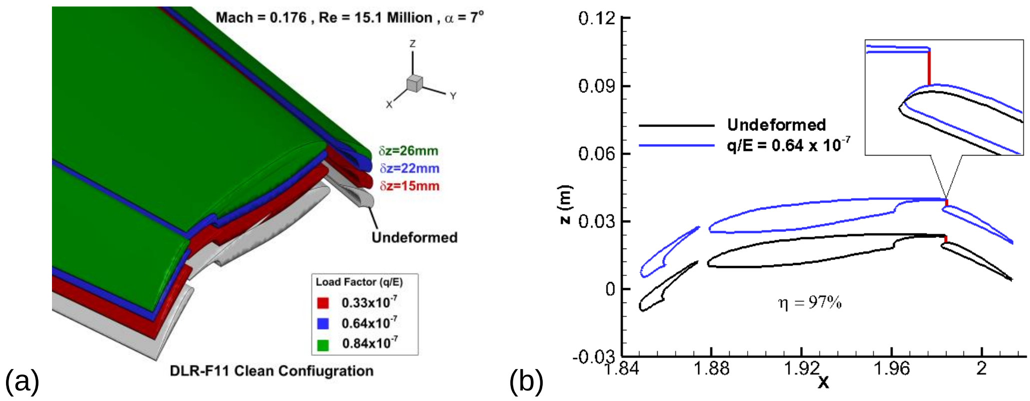

Figure 6 : Comparison of undeformed and deformed shape for clean configuration (a) Wing tip (b) Section cut at η = 97%

The gap between the main wing and the flap is reduced by approximately 10%, which was also observed in the experimental measurements. This has been illustrated in Fig. 6 (b) by overlapping the undeformed and the deformed flap section at η = 97%. The pressure distribution comparisons at two different wing sections are shown in (Figure 7 (a) and (b)).

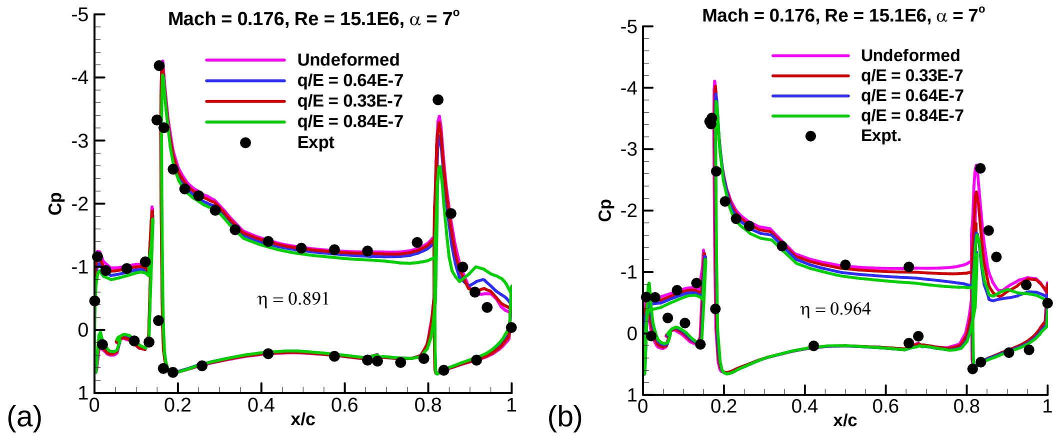

Figure 7 : Comparison of pressure distribution – load factor variation (a) η = 89.1% (b) η = 96.4%

Research civil transport aircraft (RCTA) model

The static aeroelastic analysis of RCTA model is performed at Mach number of 0.78, Reynolds number of 22 x 10^6, load factor of 0.3 x 10^{-6} and at different angles of attack. The deformed and rigid wing tip at two different angles of attack is shown in (Figure 8). The deformed state is achieved after 12 aeroelastic coupling iterations. The use of Navier-Stokes computations has shown its effectiveness in predicting the correct aerodynamic behavior at transonic flow conditions.

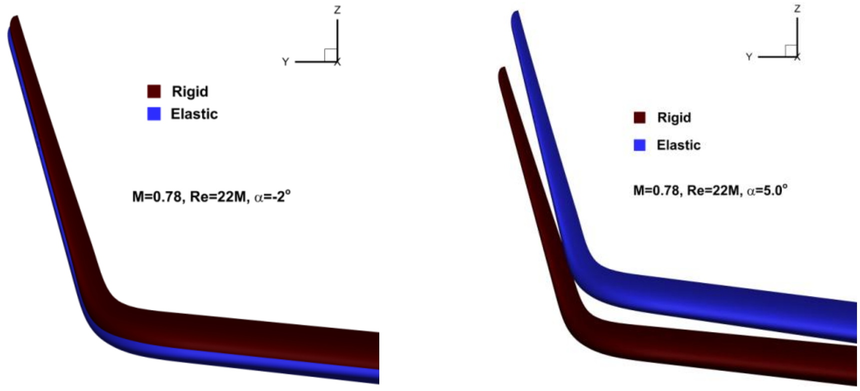

Figure 8 : Wing tip displacement comparison between rigid and elastic cases at different angles of attack

(Figure 9) shows the contour plot for pressure coefficient at Mach 0.78, Re 22 million and angle of attack 2^o. (Figure 10) shows the pressure coefficient plot at two different wing sections. It can be seen that the wing deformation has no or little effect at the wing root but it has significant effect at the wing tip and affects the aerodynamic performance of the aircraft. The present model is rigid but still the deformation has noticeable effect on the predicted values.

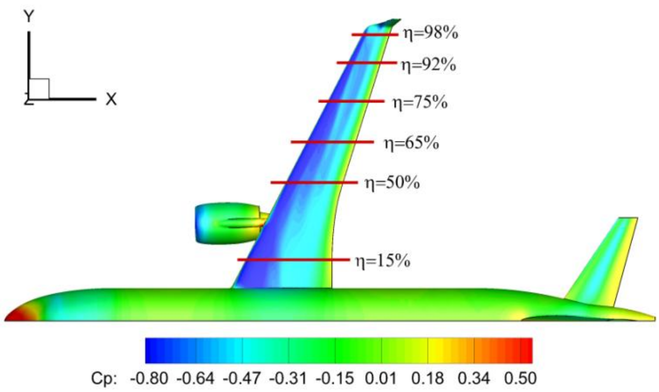

Figure 9 : Pressure distribution at α = 2^o, Mach 0.78 and Re = 22M

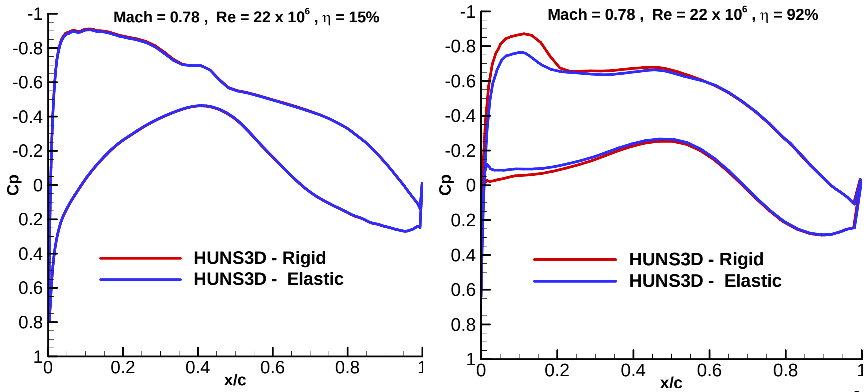

Figure 10 : Pressure Coefficient plot at two wing sections at $\alpha = 2^{o}$

The lift cure and the drag polar for the rigid and the elastic models are compared with the experimental data shown in (Figure 11). It can be seen from the figures that although the difference in the predicted coefficients for elastic and rigid model is not large but the true behavior of the lift slope has been captured when considering the elastic model.

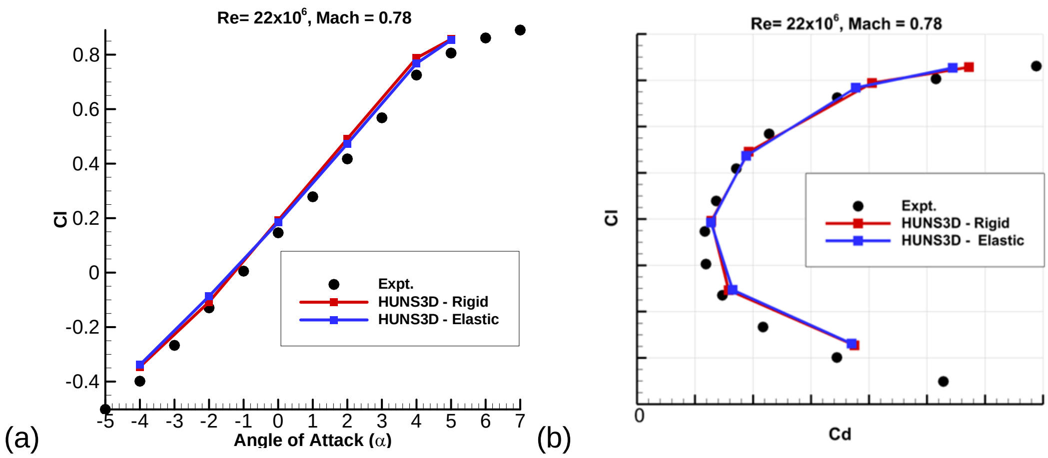

Figure 11 : (a) Lift slope curve for rigid and elastic case (b) Polar curve for rigid and elastic case

CONCLUSIONS

The paper presents the CFD/CSD coupling procedure to predict aircraft performance by taking into account aeroelastic effects. The coupling between the in-house CFD code HUNS3D and an open source finite element solver CalculiX has been performed. RBF interpolation technique serves as a robust volume mesh deformation tool which can be applied for either structured or hybrid, unstructured meshes. It has also been efficiently used for transferring aerodynamic loads and surface deformation between CFD and CSD meshes.

- It has been demonstrated that the developed fluid-structure coupled simulation approach is robust and efficient to be applied to real-life problems and it provides beneficial results in areas other than computational fluid dynamics.
- High-fidelity coupled simulations have been performed to analyze complex transport aircraft configurations including DLR-F11 high-lift model and a RCTA model. The predicted results were compared with the available experimental data and good agreement has been found.
- Although in the present case comparatively small elastic deformations are found, but their influence on chord-wise pressure distributions is clearly observable and leads to a better results for the coupled simulations.
- Even for the solid wind tunnel model the elastic nature of the structure cannot be neglected. Considerable wing deformation has been observed which influence the predicted aerodynamic coefficients.

ACKNOWLEDGEMENTS

Dr Jen-Der Lee and Dr Xiaowen Shan, Beijing Aeronautical Science and Technology Research Institute (BASTRI), COMAC, China are acknowledged for technical assistance with the wind tunnel data and for discussions involving the model deformation and comparison to computational predictions.The support from Centre of Excellence in Science & Applied Technologies (CESAT), Pakistan is acknowledged. The first author was awarded Chinese Government Scholarship from China Scholarship Council (CSC) for his MS studies and is thankfully acknowledged.

References

Batina J.T. (1991) Unsteady Euler Algorithm with Unstructured Dynamic Mesh for Complex Aircraft Aerodynamics Analysis, AIAA Journal, Vol.29 (3), p: 327-333, Mar 1991.

Bhardwaj, M. K., Kapania, R. K., Reichenbach, E., & Guruswamy, G. P. (1998) Computational fluid dynamics/computational structural dynamics interaction methodology for aircraft wings, AIAA journal, 36(12), p: 2179-2186, Dec 1998.

Bennett, R. M., and Edwards, J. W. (1998) An overview of recent developments in computational aeroelasticity, AIAA paper, AIAA-98-2421, Jun 1998.

Dhondt, G., (2012) Calculix. http://calculix.de, 2012.

Guruswamy G.P.. (2009) A New Modular Approach for Tightly Coupled Fluid/Structure Analysis, International Journal of Aerospace Innovations Vol. 1, No.1, Mar 2009.

Huo S.H., Wang F.S., Yan W.Z., Yue Z.F. (2010) Layered Elastic Solid Method for the Generation of Unstructured Dynamic Mesh, Finite Elements in Analysis and Design, Vol.46 (10), p: 949-955, Oct 2010.

Keye, S., & Rudnik, R. (2009) Aero-Elastic Simulation of DLR's F6 Transport Aircraft Configuration and Comparison to Experimental Data, AIAA Paper, AIAA 580-2009, Jan 2009.

Kirmse T., (2007) Model deformation measurements in DNW-NWB within the DLR project For-MEx. In Conference Proceedings, CD-ROM (S12–1), ODAS, 8th ONERA-DLR Aerospace Symposium, Göttingen, Germany p: 1-14, Oct 2007

Liu X., Qin N., Xia H., (2006) Fast Dynamic Grid Deformation based on Delaunay Graph Mapping , Journal of Computational Physics, Vol.211(2), p: 405-423, Jan 2006.

Mian, H. H., Wang, G., & Raza, M. A. (2013) Application and validation of HUNS3D flow solver for aerodynamic drag prediction cases. 10th International Bhurban Conference on Applied Sciences and Technology (IBCAST), IEEE, p: 209-218, Jan 2013.

Rendall T.C.S., Allen C.B. (2010) Reduced Surface Point Selection Options for Efficient Mesh Deformation using Radial Basis Functions, Journal of Computational Physics, Vol.229(8), p: 2810-2820, Apr 2010.

Rendall T.C.S., Allen C.B. (2008) Fluid-structure interpolation and mesh motion using radial basis functions, International Journal for Numerical Methods in Engineering vol 75 (10) p: 1519–1559, Jun 2008.

Rudnik R., Huber k., and Melber-Wilkending S., (2012) EUROLIFT Test Case Description for the 2nd High Lift Prediction Workshop, AIAA paper, AIAA 2012-2924, Jun 2012.

Wang G., Mian H. H., Ye Z. Y., & Lee J. D., (2013) An Improved Point Selection Method for Hybrid-Unstructured Mesh Deformation Using Radial Basis Functions, AIAA- 2013-3076, Jun 2013.

Wang G., Ye Z.Y. (2004) Mixed Element Type Unstructured Grid Generation and its Application to Viscous Flow Simulation, 24th International congress of aeronautical sciences, Jun 2004.

Wang G.., Jiang Y., Ye Z.Y. (2012) An Improved LU-SGS Implicit Scheme for High Reynolds Number. Flow Computations on Hybrid Unstructured Mesh, Chinese Journal of Aeronautics vol25, p: 33-41, Feb 2012.

2nd AIAA CFD High Lift Prediction Workshop (2013) (HiLiftPW-2), ttp://hiliftpw.larc.nasa.gov/, Jun 2013